JOURNAL OF THERMOPHYSICS AND HEAT TRANSFER
Vol. 17, No. 4, October–December 2003

Thermal Operational Characteristics of a Small-Loop Heat Pipe

Tarik Kaya*
Carleton University, Ottawa, Ontario K1S 5B6, Canada
and
Jentung Ku†
NASA Goddard Space Flight Center, Greenbelt, Maryland 20771

This study investigates the distinctive thermal operational characteristics of a small-loop heat pipe (LHP). Tests are conducted under varying heat load and condenser sink temperatures at different orientations of the LHP. Successful startups at heat loads as low as 5 W are demonstrated. To investigate the effect of accelerating forces, the small LHP is tested on a spin table. Accelerating forces impose an additional pressure drop and change the fluid distribution inside the LHP, thereby affecting the startup characteristics and the LHP operating temperature. Spin tests have demonstrated successful operation of the LHP under accelerating forces. The steady-state mathematical model proves to be useful for assessment of the main factors influencing the operating temperature when the LHP is subjected to accelerating forces. The mathematical modeling of the LHP performance characteristics becomes more difficult as the size of the LHP decreases. For a better prediction of the small LHP characteristics, more detailed modeling of the evaporator core is essential.

Nomenclature

a	=	acceleration, m/s^2
Bo	=	Bond number
c_p	=	specific heat at constant pressure, J/(kg-K)
D_W^i	=	inner diameter of wick, m
D_W^o	=	outer diameter of wick, m
k_W	=	thermal conductivity of wick material, W/(m-K)
L_e	=	effective length of evaporator, m
L_W	=	length of wick, m
$\dot{m}$	=	mass flow rate, kg/s
$\dot{Q}_{\mathrm{HL}}$	=	heat leak, W
r_p	=	effective pore radius of wick, m
UA	=	overall thermal conductance of wick, W/K
ΔP_{ACC}	=	pressure drop caused by accelerating forces, Pa
ΔP_W	=	pressure drop across wick, Pa
ΔT_W	=	temperature difference across wick, K
ρ	=	density of working fluid, kg/m^3
σ	=	surface tension of working fluid, N/m

I. Introduction

As the power density of modern electronic equipments is steadily increasing, innovative thermal control techniques with miniaturization potential are gaining more attention from the industry. Among the available techniques two-phase capillary thermal control devices are specially promising. Heat pipes have been used in many applications for electronics cooling, such as notebook computers, since the mid-1990s.[1] More recently, the advanced micro-heat pipes have been proposed for other applications such as spacecraft thermal control for human missions to Mars.[2] Loop heat pipes (LHPs) alternatively offer many advantages over heat pipes in terms of operability against gravity, the maximum heat-transport capability, smooth-walled flexible transport lines, and fast diode action. The LHP is a passive thermal transport device, which uses the surface tension forces formed in a fine-pore wick to circulate the working fluid. After the disclosure of the design characteristics by Maidanik et al.[3] in 1985, LHPs have become an important research area in both space and ground applications. Detailed description of the working principles of the LHPs can be found in Refs. 4 and 5.

The earlier LHPs were mainly designed for high-power applications on the order of 1 kW. Because there is strong interest to design smaller spacecraft primarily to reduce the mission cost, the current LHP designs are trying to respond this miniaturization trend in the space industry. Miniature LHPs can also offer efficient design solutions for increasingly demanding cooling requirements of modern microprocessors for high-end electronic devices. Design of a LHP with an outer evaporator diameter of less than 12 mm is a challenge. The main technical difficulties include manufacturing the evaporator, inserting the wick into the evaporator core, and welding thin-walled transport lines with diameters less than 2 mm. On the operational side, establishing the required temperature difference across a wick with small characteristic dimensions is also difficult.[6] A miniature LHP should also satisfy a tight temperature requirement and operate against gravity in order to maintain the advantage of ground testability at any orientation.

Miniaturization of LHPs is therefore a current research topic of industrial importance. The number of publications in open literature on small LHPs is limited. Pastukhov et al.,[6] Bienert et al.[7] and Figus et al.[8] have presented different aspects of the small LHPs. Maidanik et al.[9] claimed that it was realistic to manufacture cylindrical evaporators with an outer diameter of 4 mm and flat evaporators with a thickness of 8 mm. In a further smaller scale micromachined silicon LHP development was also attempted for on-chip electronic cooling by using technology of microelectromechanical systems (MEMS).[10] Introduction of the LHPs into industries other than the aerospace industry has been slow because of their high manufacturing cost. Research is however underway to produce low-cost wicks and manufacturing techniques.[11] It is therefore becoming feasible that inexpensive and miniature LHPs will be implemented into many advanced products in the foreseeable future.

In this study thermal operational characteristics of a small LHP were experimentally investigated. The tests focused on startup and shutdown characteristics and the LHP's response to rapidly varying power and sink cycles. The small LHP was also installed on a spin table to investigate the effect of accelerating forces on the LHP operational characteristics. The main purpose of these spin tests was to simulate certain applications such as spin-stabilized spacecraft, maneuvering in space for orbit and attitude control, or rapidly maneuvering military ground vehicles. The experimental results were

Received 3 September 2002; revision received 31 March 2003; accepted for publication 21 April 2003.

*Assistant Professor, Department of Mechanical and Aerospace Engineering; tkaya@mae.carleton.ca.
†Group Leader; jku@mscmail.gsfc.nasa.gov.

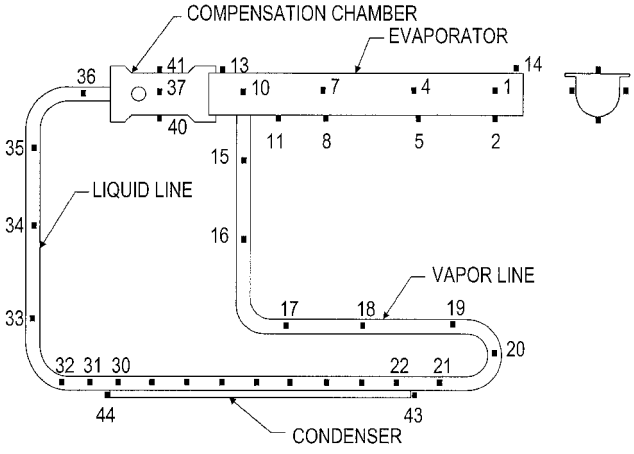

Fig. 1 Schematic of the small LHP in the horizontal position and thermocouple locations (not to scale).

also compared with the mathematical calculations obtained by using a steady-state model.

II. Test Article and Experimental Setup

A. Test Article

The test article used for this study was a small LHP with a weight of less than 150 g. This LHP was constructed primarily of aluminum, and its working fluid was ammonia. Because of its small mass and size, this LHP can easily be tested at various configurations on the ground. It can also easily be mounted on a spin table to investigate the effect of different acceleration patterns. A reference coordinate system fixed to the spin table was used to describe different orientations of the LHP. The spin axis was chosen as the Z axis of the coordinate system. The Z axis was parallel to the gravity vector and towards the opposite direction of gravity. The X axis was aligned with the radial direction of the spin table. The Y axis completed the coordinate system and was perpendicular to the XZ plane. The small LHP in the horizontal position and the thermocouple locations are shown in Fig. 1. The thermocouples located on the other side of the evaporator and the compensation chamber are not shown in this figure.

This LHP had a cylindrical evaporator with an outer diameter of 13 mm, an inner diameter of 10 mm, and a length of 120 mm. The evaporator used a sintered nickel wick with an effective pore radius of less than 1.2 μ. The nickel wick was inserted into the aluminum body. The wick had an outer diameter of 10 mm and an inner diameter of 4 mm. The permeability of the nickel wick was 4×10^{-14} m^2 with 60% porosity. The compensation chamber had an outer diameter of 13 mm, an inner diameter of 10 mm, and a length of 30 mm. The transport lines and condenser were machined from the same aluminum extrusion. Both the liquid and vapor transport lines and condenser had an outer diameter of 3.8 mm and an inner diameter of 2.5 mm. The lengths of the liquid line and the vapor line were 130 and 160 mm, respectively. The condenser was a single-pass, direct-condensation heat-exchanger type with a total length of 100 mm.

B. Experimental Setup

A copper saddle was attached to the evaporator flange to hold a cartridge heater with a maximum heating capability of 500 W. Thermal grease was used as the interface material between the heater block and the evaporator flange. The uncertainty in measuring the power input was estimated to be less than 2%.

Similar to the evaporator section, a copper block was attached to the condenser section of the LHP. Two parallel cooling lines were embedded inside the condenser copper block. The cooling lines were connected to a refrigerator with a 1.5-kW cooling capacity. The heat-rejection system was able to maintain the sink temperature within ± 1 K of the chosen set point. The entire LHP was insulated with 15-mm-thick Armaflex material to minimize parasitic heating.

Temperatures of the LHP at various locations and ambient were measured by 50 copper/constantan (type T) thermocouples (Fig. 1). The uncertainty of the thermocouple readings was estimated to be less than ± 0.5 K.

The sampling rate of data-acquisition system was set to 10 kHz with a resolution of 16 bit. The accuracy of the data-acquisition system was calculated to be 0.6%.

A spin table was used to investigate the operational characteristics of the LHP under accelerating forces. The spin table consisted of a motor, a speed reducer, three slip rings, and two spinning arms on opposite sides of the rotating axis, each about 1300 mm long. The LHP was mounted at the end of one of the arms. The temperature values were collected on a data logger mounted to the spin table. The output from this data logger was fed through three slip rings to the data-acquisition system. An accelerometer was used to measure either radial or tangential acceleration while the system was spinning. The uncertainty in measuring the accelerations was estimated to be less than 1.5%. A tachometer mounted on the stationary portion of the spin table was also used to measure the speed of rotation within 2% accuracy. To cool the LHP during a spin test, two separate coolant-circulating loops were employed. The first stationary loop delivered the coolant from the refrigerator to an intermediate reservoir, which was mounted around the spin axis. The second loop, which rotated with the test article, delivered coolant from the reservoir to the LHP condenser. A mechanical pump was used to circulate coolant. Design details of the experimental setup with the spin table can be found in Refs. 12 and 13.

III. Discussion of Results

A. Stationary Tests

The small LHP was first tested under a stationary condition. These stationary tests were focused on the identification of the distinctive characteristics of a small LHP. Startup at low heat loads was of primary importance. The LHP was tested at different orientations relative to the gravity vector, as well as under rapidly varying heat load and sink conditions.

Startup and Power Cycle

Small LHPs are designed for low heat load applications. Therefore, they must be able to start with low startup power levels because additional starter power might not be available in these types of applications. In any case the use of starter heaters is not desirable because of the added complexity and decreased reliability of the system. Applications with large thermal masses might however require startup heaters especially if the mission requires a rapid startup. Particularly, in space applications where long waiting period or risk of no startup cannot be tolerated, the use of starter heaters needs to be taken into account in the system-level design.[14]

To investigate the low power startup characteristics of this LHP, a power level of 5 W was chosen. Several startups were attempted at different sink temperatures and the LHP orientations. Figure 2 represents a typical startup when the LHP was in horizontal position. The number of the thermocouples used in the figures is given in parentheses. The LHP was leveled within ± 1.0 mm from one end to the other in the horizontal XY plane. The sink temperature was 270 K. The LHP was started almost immediately after the power was applied. This could be seen by the sudden increase of the vapor line temperatures. Prior to the startup, the vapor grooves were probably filled with two-phase fluid because there was no noticeable superheat at the onset of the startup. The compensation chamber temperatures closely followed the evaporator temperatures, indicating that the evaporator core also contained two-phase fluid prior to the startup. After the startup the temperatures first increased and then dropped towards their steady-state equilibrium values determined by the imposed conditions on the LHP. This is commonly referred as temperature overshoot. This temperature overshoot was caused by the slow movement of cold liquid from the condenser. The liquid line was originally warm, and it took some time for the cold liquid from the condenser to reach the compensation chamber. When the power input was increased to 10 W, the saturation temperature in the LHP decreased as a result of the increased conductance

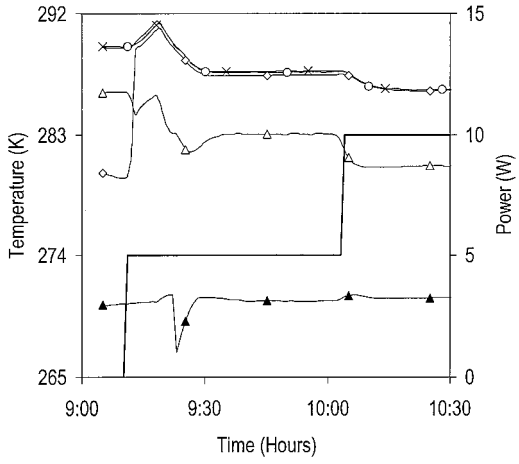

Fig. 2 Temperature profiles during startup. Thermocouple numbers in parentheses: ○, evaporator (8); ×, compensation chamber (37); ◇, vapor line (16); △, liquid line (35); ▲, condenser (43); and ——, power.

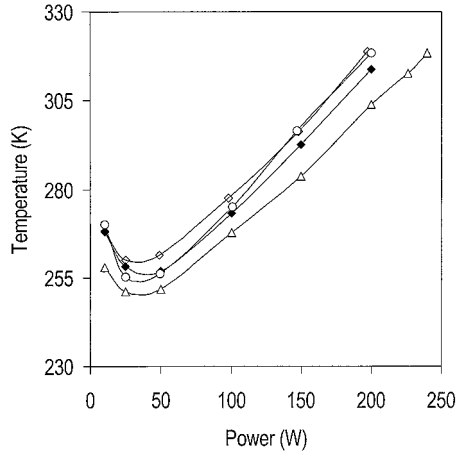

Fig. 3 Performance curves at different LHP orientations: △, horizontal; ◇, compensation chamber above evaporator; ○, evaporator above compensation chamber; and ♦, evaporator above condenser.

as shown in Fig. 2. As the vapor–liquid interface has not reached the end of the condenser yet, this result was typical for the variable conductance operation of a LHP.

Several startup tests were performed at other LHP orientations to investigate the effect of the gravitational force. These orientations were compensation chamber above evaporator, evaporator above compensation chamber, and condenser above both the evaporator and compensation chamber. In these orientations the LHP was maintained in a vertical XZ plane within ± 1.0 mm. All of the tests were conducted with a sink temperature of 233 K. Each one of the 5-W startup attempts was successful. After a successful startup, the LHP was tested by increasing heat load in steps. The resulting performance curves were shown in Fig. 3. The results represent the average temperature of the six thermocouples placed around the compensation chamber. The curves displayed typical variable and fixed-conduction operation regions with a distinctive minimum operating temperature. The variable conductance operation was extended up to about 40 W, and its exact location changed slightly depending on the LHP orientation. Depending on the LHP design, the descending part of the performance curve in the variable conductance region is sometimes highly sensitive to the changes in orientation.[15,16] In our case the performance curves were similar in shape regardless of the orientation.

During the power cycling tests, the temperature hysteresis characteristics of the small LHP were also investigated. The temperature hysteresis was identified by the fact that the operating temperature depends upon not only the imposed power but also the previous

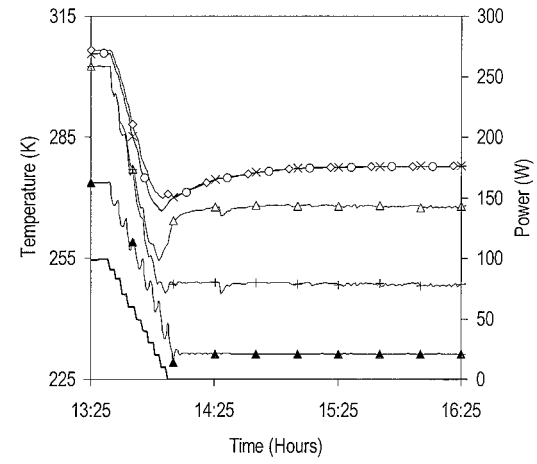

Fig. 4 Temperature profiles under rapidly varying heat load and sink conditions. Thermocouple numbers in parentheses: ○, evaporator (8); ×, compensation chamber (37); ◇, vapor line (16); +, liquid line upstream (32); △, liquid line downstream (35); ▲, condenser (43); and ——, power.

history of the power variation. There is strong evidence that the temperature hysteresis is directly related to the void fraction of the evaporator core. A large decrease in applied power seems to modify the core void fraction, leading to different operating temperatures at the same power level by changing the amount of heat leak.[17] Ku et al. explained in detail how the void fraction directly affected many aspects of the LHP operation in Ref. 18. To investigate the possible temperature hysteresis characteristics caused by the rapid power change, the LHP power was cycled with large steps (5 W/200 W/5 W). For this power cycle no temperature hysteresis was observed during the stationary tests. As it was reported in Ref. 17, the temperature hysteresis strongly depends on the individual LHP design. It is not systematically observed when a LHP is subjected to a sudden power decrease. The true mechanism of the temperature hysteresis has not been well understood.

The small LHP was also tested under rapidly varying heat load and sink conditions. The main purpose of these tests was to simulate conditions such as spacecraft entering into the eclipse in a planetary orbit. For these tests the power was decreased from 100 to 0 W with increments of 10 W about every 3 min, while the sink temperature was decreased from 273 to 233 K with increments of 5 deg about every 4 min. A typical test result is shown in Fig. 4. As the power and sink temperature decreased, the LHP temperatures dropped accordingly. The rapid changes in power and condenser sink temperature did not have any negative effect on the performance of the LHP.

An interesting result observed during this test was that the LHP continued its operation even after the power was reduced to 0 W while the sink temperature was maintained at 233 K. The parasitic heating from environment through convection was sufficient to sustain a steady flow. As shown in Fig. 4, the LHP operation was stable under 0 W. The test condition was successfully maintained for more than 20 h before the test was intentionally ended. Similar tests performed with different power cycles and the LHP orientations showed that after a successful startup, it was difficult to shut down a small LHP by removing the heat load in convection environment caused by the parasitic heating. In the case of space flight, the attached thermal mass could provide parasitic heating. In a similar mode this parasitic heating might delay the shutdown under no load conditions. For a safe shutdown it is therefore necessary to heat the compensation chamber at a faster rate than the evaporator to ensure that the circulation inside the LHP stops.

Mathematical Model

A steady-state mathematical model, previously developed and presented in Refs. 19 and 20, was modified to predict the operating temperatures of this small LHP. This model was based on the steady-state energy conservation equations and the two-phase pressure drop

calculations along the fluid path inside the LHP. In this model it was assumed that the space formed by the evaporator core and compensation chamber contains two-phase fluid at all times. At a given LHP condition the model predicts the steady-state LHP operating temperature as a function of the applied power.

The calculation of the heat exchange between the environment, and the transport lines and compensation chamber is a difficult task in modeling the LHP operation although it might seem to be a secondary effect. Earlier articles on the LHP modeling (Refs. 21 and 22) also addressed this difficulty. The heat exchange with the surroundings becomes even more important for small LHPs. This is because of the low mass-flow rates associated with the low power levels in the small LHPs as the fluid particles have longer dwelling times in the transport lines in spite of the smaller diameter tubes. Furthermore, the heat and mass transfer in small diameter tubes is not sufficiently investigated. Empirical correlations for natural convection are however available in the literature for the Rayleigh numbers as low as 10^{-10}. Two such correlations from Refs. 23 and 24 were incorporated to the mathematical model in an attempt to better simulate tubes with smaller dimensions.

In the calculation of the heat leak, the radial mass flow, which was neglected in the steady-state mathematical model just mentioned, was also taken into account in addition to the radial heat conduction. The heat-leak equation thus takes the following form:

$$\dot{Q}_{\mathrm{HL}} = \dot{m} c_p \left[\frac{\Delta T_W}{\left(D_W^o / D_W^i \right)^{\dot{m} c_p / 2\pi k_w L_w} - 1} \right] \tag{1}$$

The effect of radial mass flow was less than expected. An improvement of up to 5% was obtained at the high power region. Figure 5 represents the comparison of the mathematical predictions and experimental results for a sink temperature of 233 K. The experimental results represent the average temperature of the six thermocouple measurements around the compensation chamber. The ambient temperature during the test was 293 K. The LHP was placed in the horizontal XY plane. The predictions were within 8.5 deg of the experimental measurements as shown in Fig. 5. Agreement was less satisfactory than those obtained for larger LHP designs. The prediction of the LHP characteristics becomes more difficult as the dimensions of the LHP decrease. Better correlation and modeling are necessary for more accurate prediction of the small LHP performance characteristics.

B. Spin Tests

The main objective of the spin tests was to study the effect of different accelerating forces on the LHP operation, mainly the startup and operating temperature characteristics. As the test unit was small, the variation of accelerating forces from one end of the LHP to the other was less than 15%. Tests were conducted at two different rotational speeds, 30 and 60 rpm. The corresponding accelerations

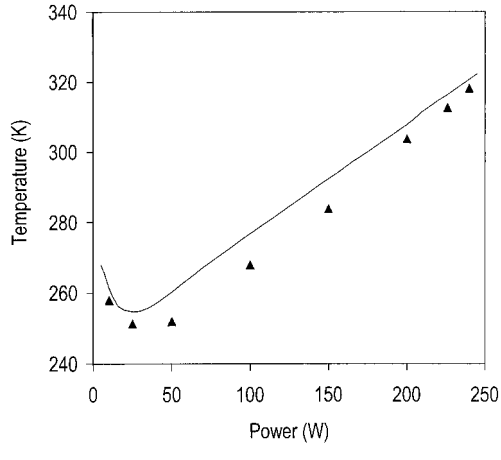

Fig. 5 Comparison of experimental results and model predictions: ▲, measurements and ——, predictions.

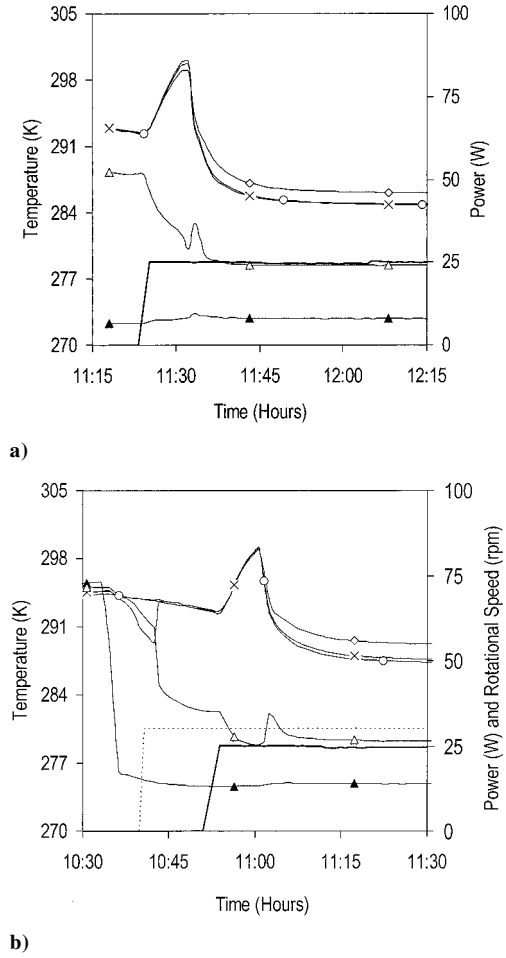

Fig. 6 Temperature profiles at startup: a) stationary test and b) spin test. Thermocouple numbers in parentheses: ○, evaporator (8); ×, compensation chamber (37); ◇, vapor line (16); △, liquid line (35); ▲, condenser (43); ——, power; and - - - -, rotational speed.

calculated at the midpoint of the LHP were 1.2 and 4.8 g, respectively. The LHP was tested at different orientations relative to the direction of accelerating force by varying the startup power and condenser sink temperature. Test results were also compared with the numerical predictions.

Startup

Figure 6 represents two typical startups with a power of 25 W and sink temperature of 273 K. Figure 6a was obtained during a stationary test without spin. For the stationary tests the LHP was located on the vertical XZ plane with the compensation chamber below the evaporator. For the spin tests the LHP was placed on the horizontal XY plane with the axis of the evaporator parallel to the X direction and the compensation chamber on the far end of the spin table. This configuration was similar to the just-mentioned stationary configuration that the fluid would be pushed away from the evaporator towards the compensation chamber, imposing more load on the secondary wick. Figure 6b represents the results obtained during a spin test. The LHP was rotated with 30 rpm before applying power to the evaporator. Resulting fluid shift in the vapor and liquid lines could be easily seen in Fig. 6b by the sudden change of temperature measurements. The liquid line temperature was suddenly decreased by the colder liquid pushed out of condenser towards the liquid line, and the vapor line temperature was increased by the warmer liquid pushed out of the evaporator towards the vapor line as a result of the spinning action. The startup parameters were nearly identical for both cases. As shown in Figs. 6a and 6b, the LHP started just after the power was applied to the evaporator. The startup must have been initiated by surface evaporation process, not by pool boiling, in the evaporator grooves. The temperature overshoots observed for both

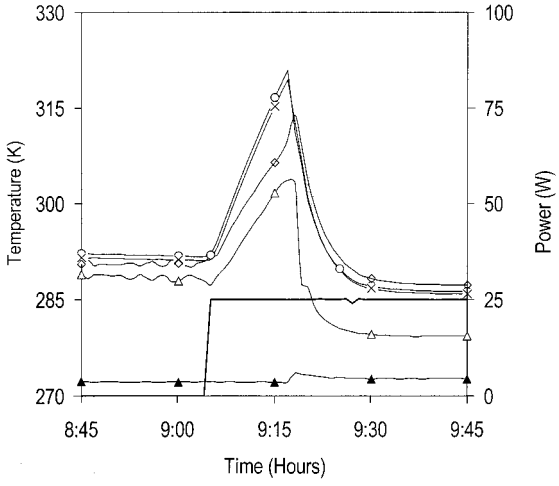

a)

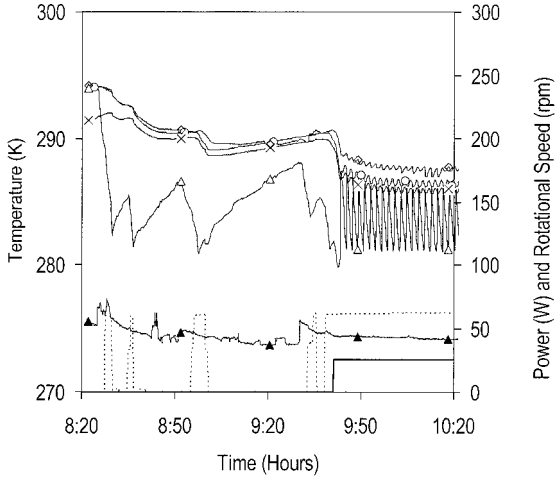

b)

Fig. 7 Temperature profiles at startup: a) stationary test and b) spin test. Thermocouple numbers in parentheses: ○, evaporator (8); ×, compensation chamber (41); ◇, vapor line (16); △, liquid line (35); ▲, condenser (43); ——, power; and - - - -, rotational speed.

cases were caused by time delay required for the subcooled liquid to reach the compensation chamber.

Note that in Figs. 6a and 6b the vapor line temperatures were warmer than the evaporator and compensation chamber temperatures. This was caused by the parasitic heating of the vapor lines because the LHP operating temperature at these test conditions was less than the ambient temperature.

To verify the preceding conclusions, the LHP was repositioned on the same horizontal XY plane. The axis of the evaporator was again parallel to the X direction; however, the compensation chamber was moved closer to the spin axis. In this configuration the fluid would be pushed from the compensation chamber to the evaporator under the influence of the spinning action. To compare these results with the similar static case, the LHP was first tested without spin when the compensation chamber was above the evaporator in the vertical XZ plane. Figure 7a represents the startup at static conditions with a power of 25 W and sink temperature of 273 K. A significant temperature overshoot was observed. The compensation chamber temperatures rose up to 319 K, 23 deg more than the final steady-state operating temperature. The LHP started approximately 12 min after the power was applied. The test results indicated that the evaporator core contained two-phase fluid prior to the startup and the evaporator grooves were liquid filled. The pool boiling was the main mechanism for the startup. It took some time to establish the required temperature difference between the compensation chamber and evaporator for boiling, leading to the temperature overshoot. This mechanism for temperature overshot was different from the just-mentioned one caused by the slowly moving cold liquid.

The excess temperature or superheat required for pool boiling is difficult to measure in a LHP. The temperature overshoot strongly depends on the superheat. Ku et al.[12] performed an extensive survey on the nature of superheat for different test configurations based on the wall temperature measurements. They could not find any apparent pattern and concluded that superheat and temperature overshoots were stochastic. The amount of superheat depends, in a complicated manner, on many parameters including applied power, thermophsyical properties of fluid, dynamics of vapor bubble formation, and subsequent vapor bubble detachment from the wall.

For the dynamic tests at this configuration, the LHP was subjected to a random spinning pattern prior to startup to simulate an arbitrary vehicle motion as shown in Fig. 7b. The LHP was then rotated at a constant speed of 60 rpm prior to applying power. The startup was immediate. The startup was initiated by the surface evaporation. The accelerating force must have produced a vapor–liquid interface in the evaporator grooves by pushing off fluid from the grooves. The random spinning action also pushed cold liquid from condenser into the liquid lines as shown in Fig. 7b. As a result, no temperature overshoot was observed immediately after the startup. The temperature fluctuations, shown in Fig. 7b, were caused by the vapor–liquid front reaching the end of the condenser. In such a case the vapor–liquid front moves back and forth around the condenser exit, and the LHP operating temperature starts oscillating. A detailed discussion of this mechanism can be found in Ref. 25.

Other startups performed at different sink and power conditions indicated that the LHP had sufficient capillary force for successful startups up to 4.8 g regardless of the direction of acceleration. In majority of the cases, high accelerating forces decreased the required temperature overshoot prior to startup by creating a vapor–liquid interface in the vapor grooves. Temperature overshoots were also smaller or absent at high startup powers. This was for two reasons. First, at high powers there was enough power available to heat the fluid in the evaporator grooves at a faster rate than the compensation chamber. Evaporation therefore took place quickly without important temperature overshoot. Second, because of the high mass-flow rates at high powers subcooled liquid arrived at the compensation chamber at a faster speed. Therefore, the LHP reached its equilibrium point without experiencing high temperatures.

Because the rotational speed of the spin table was limited to 60 rpm during these tests, the LHP could not be tested at higher accelerating forces. At higher spin rates the accelerating force can overcome the pumping capacity of the secondary wick, causing a dryout of the primary wick. By using a copper-water heat pipe, Ponnappan et al.[26] have shown that the dryout limit decreased with increasing radial acceleration. For a given acceleration rate it was however possible to reprime the heat pipe by reducing the heat load. Kiseev et al.[27] were able to impose a radial acceleration of 10 g on a LHP without experiencing deprime. By using different working fluids, they have found that the LHP deprimed when the Bond number ($Bo = \rho a L_e r_p / 2\sigma$) was greater than unity. In our case the highest Bond number was 0.06, and no deprime was observed during the spin tests.

LHP Operating Temperature

The accelerating forces produced on the spin table affected the steady-state LHP operating temperature by imposing additional pressure drop and by changing the fluid distribution inside the LHP. Table 1 summarizes the operating temperatures obtained at different powers and sink temperatures as a function of different accelerating forces. For these tests the LHP was leveled on the horizontal XY plane, and the evaporator axis was parallel to the X axis. The compensation chamber was on the far edge of the spin table. The analogous stationary case in Table 1 refers to the results obtained when the evaporator was placed above the compensation chamber on the vertical XZ plane. In Table 1 the calculated operating temperatures were also presented for the available test cases. Table 2 represents the similar results obtained when the LHP was placed on

Table 1 Comparison of measured and calculated operating temperature values at different power and sink temperature settings as a function of acceleration rates

		Rotational acceleration, m/s^2						
		1 *g*		1.2 *g*		4.8 *g*		
		Operating temperature, K						Analogous stationary case, K
Power, W	Sink temperature, K	Measured	Calculated	Measured	Calculated	Measured	Calculated	
25	273.0	285.9	**285.4**	286.4	**285.4**	292.4	**287.6**	No data
100	273.0	312.7	**310.3**	305.5	**310.3**	305.9	**310.0**	315.0
100	233.0	281.2	**280.6**	276.4	**280.3**	275.6	**278.4**	No data

Table 2 Comparison of measured and calculated operating temperature values at different power and sink temperature settings as a function of acceleration rates

		Rotational acceleration, m/s^2						
		1 *g*		1.2 *g*		4.8 *g*		
		Operating temperature, K						Analogous stationary case, K
Power, W	Sink temperature, K	Measured	Calculated	Measured	Calculated	Measured	Calculated	
25	273.0	284.0	**285.4**	285.1	**286.0**	286.8	**288.5**	No data
100	273.0	314.0	**310.3**	314.5	**310.3**	314.2	**310.6**	318.2
100	233.0	281.3	**280.6**	283.3	**281.0**	282.1	**280.2**	No data

the horizontal XY plane, and the compensation chamber was closer to the spin axis.

An accurate prediction of the operating temperature as a function of the spin rate is a complex task caused by many interrelated factors, and the steady-state mathematical model is not elaborated enough to make accurate predictions. Therefore, the mathematical model was used only to identify the main factors influencing the LHP operating temperature under accelerating forces, and the model was useful in determining the trend of the operating temperature. As it can be shown in Tables 1 and 2, the calculations correctly simulated increasing and decreasing trends of the operating temperatures for different settings. Comparison of the measurements and calculations indicated that there were four interrelated main factors influencing the LHP operating temperature. The final operating temperature depended on the combination of these four factors:

1) The first factor is the pressure drop inside the LHP. The heat leak from the evaporator to the compensation chamber can be calculated by the following equation:

$$\dot{Q}_{\mathrm{HL}} = (UA)\left(\frac{\partial T}{\partial P}\right)_{\mathrm{SAT}} (\Delta P_W \pm \Delta P_{\mathrm{ACC}}) \tag{2}$$

where $(\partial T/\partial P)_{\mathrm{SAT}}$ is the slope of the vapor–pressure curve and is a function of the operating temperature. The overall thermal conductance across the wick UA depends on the state of the evaporator core. It is clear from Eq. (2) that the heat leak will increase if the pressure drop caused by the accelerating forces ΔP_{ACC} contributes positively to the total pressure drop. ΔP_{ACC} depends on the spin configuration and the location of the vapor–liquid interface in the condenser. The interface position in turn depends on the inertial, accelerating, and surface tension forces. It can be seen in Tables 1 and 2 that the change in operating temperature was much smaller when the condenser was fully open at 100 W/273 K because an open condenser means smaller hydrostatic pressure. For high heat loads such as 100 W, ΔP_{ACC} became a small portion of the total pressure drop inside the LHP. This would also decrease the influence of ΔP_{ACC} on the heat leak.

2) The second factor is the state of the evaporator core. The heat leak directly depends on the state of the evaporator core. If the void fraction of the evaporator core is higher, the overall thermal conductance across the wick UA will be larger and according to Eq. (2), the heat leak will increase, leading to higher operating temperatures. The determination of UA is a major difficulty in modeling the LHPs. The mathematical model used in this study employed standard correlations for the prediction of the effective thermal conductance across the wick.[20] The differences between the measured and calculated LHP operating temperatures were mainly attributed to the inability to predict the overall effective thermal conductance across the wick.

3) The third factor is the heat-transfer coefficient in the condenser. The spinning action directly influenced the condenser heat-transfer coefficient and thus subcooling of the returning liquid. This in turn affected the operating temperature, which was mainly determined by the energy balance between the heat leak and liquid subcooling. At 0 rpm the liquid pooled at the bottom, and the condensate film thickened, leading to higher thermal resistance. When the spin rate increased, the liquid condensate film became thinner, increasing the heat-transfer coefficient. This mechanism did not play any role when the condenser was fully utilized, as shown in Tables 1 and 2 for 100 W/273 K setting. The decrease in the operating temperatures for 100 W/233 K setting was attributed to the dominant role of increased heat-transfer efficiency in the condenser. For 25 W/ 273 K setting, as a result of the smaller mass flow associated with the lower heat load, the increase in the condenser heat transfer efficiency caused by the spin was not sufficient to offset other effects to decrease the operating temperature.

4) The last factor is the heat-transfer coefficient between the LHP and environment. The change in heat exchange with surroundings caused by the spinning action was calculated by using a correlation suggested in Nakai and Okazaki.[28] An increase in overall heat-transfer coefficient with ambient up to 8.5% was observed at 60 rpm with respect to the stationary case. However, the overall effect on the LHP operating temperature was much less. This effect becomes more important if there is a large difference between the LHP operating temperature and ambient temperature.

An accurate prediction of the operating temperature under accelerating forces is quite complex. The operating temperature of the LHP will be determined depending on which one of the preceding factors is more important. If tight temperature limits are required for a specific application, the active control of the operating temperature might then be necessary. Bienert et al.[7] have demonstrated that the operating temperature of a similar small LHP could be maintained within less than ± 0.25 deg by using very low control power. To increase the stability of the LHP operation, they applied the control power to the liquid line instead of the more common method of heating the compensation chamber. It now needs to be demonstrated that the operating temperature can be controlled within desired limits by

using this technique even when the LHP is subjected to randomly varying accelerating forces.

IV. Conclusions

Experimental investigation of a small LHP was performed to demonstrate the successful operation under varying heat loads and condenser sink temperatures and different LHP orientations. The LHP successfully started with heat loads as low as 5 W. It was observed that the small LHP could continue to operate for long time because of the parasitic heating, even after the applied power was removed. To ensure a safe shutdown, it is therefore necessary to heat the compensation chamber at a faster rate than the evaporator. Heat exchange with surroundings plays a significant role for the small LHPs as a result of the low mass-flow rates associated with the low heat loads. The calculated operating temperatures compared well with experimental results. However, the model predictions were less satisfactory than those obtained for larger LHP designs.

All of the startup attempts were successful when the small LHP was tested on a spin table. Accelerating forces affected the superheat for boiling and the temperature overshoot values prior to startup in an unpredictable way. If a specific application does not tolerate potential temperature overshoots at startup, use of small startup heaters is recommended. Accelerating forces also affected the LHP operating temperature by imposing an additional pressure drop and by changing the fluid distribution inside the LHP. The steady-state mathematical model was a useful tool in identifying the main factors influencing the LHP operating temperature under accelerating forces. Accurate prediction of the operating temperature as a function of accelerating forces is a complex task. Prediction of the state of the evaporator core and the overall thermal conductance across the wick are crucial for a better modeling of the LHP behavior. Future investigation will focus on more realistic modeling of the evaporator region.

Acknowledgments

This work was jointly funded by NASA Goddard Space Flight Center, U.S. National Research Council, and U.S. Army Tank-Automotive Research Development and Engineering Center. The financial support of CRESTech (Centre for Research in Earth and Space Technology) is also acknowledged. The experimental work was performed at NASA Goddard Space Flight Center.

References

[1]Xie, H., Aghazadeh, M., Liu, W., and Haley, K., "Thermal Solutions to Pentium Processors in TCP in Notebooks and Sub-Notebooks," *IEEE Transactions on Components, Processes and Manufacturing, Part A*, Vol. 19, No. 1, 1996, pp. 54–65.

[2]Wang, Y. X., Ma, H. B., and Peterson, G. P., "Investigation of the Temperature Distribution on Radiator Fins with Micro Heat Pipes," *Journal of Thermophysics and Heat Transfer*, Vol. 15, No. 1, 2001, pp. 42–49.

[3]Maidanik, Y. F., Vershinin, S., Kholodov, V., and Dolggirev, J., "Heat Transfer Apparatus," U.S. Patent 4515209, May 1985.

[4]Maidanik, Y. F., Fershtater, Y. F., and Solodovnik, N. N., "Design and Investigation of Regulation of Loop Heat Pipes for Terrestrial and Space Applications," Society of Automotive Engineers, Paper 941407, June 1994.

[5]Ku, J., "Operational Characteristics of Loop Heat Pipes," Society of Automotive Engineers, Paper 1999-01-2007, July 1999.

[6]Pastukhov, V. G., Maidanik, Y. F., and Chernyshova, M. A., "Development and Investigation of Miniature Loop Heat Pipes," Society of Automotive Engineers, Paper 1999-01-1983, July 1999.

[7]Bienert, W. B., Krotiuk, W. J., and Nikitkin, M. N., "Thermal Control with Low Power, Miniature Loop Heat Pipes," Society of Automotive Engineers, 1999-01-2008, July 1999.

[8]Figus, C., Puillet, C., and Supper, W., "Development of Miniaturised Fluid Loops in Astrium," International Two-Phase Thermal Control Technology Workshop, The Aerospace Corp., El Segundo, CA, June 2001.

[9]Maidanik, Y. F., Vershinin, S. V., Pastukhov, V. G., Chernysheva, M. A., and Sudakov, R. G., "Generalization of the Experience of Development and Tests of Miniature LHP's with a Cylindrical and a Flat Evaporator," International Two-Phase Thermal Control Technology Workshop, The Aerospace Corp., El Segundo, CA, June 2001.

[10]Hoelke, A., Henderson, H. T., Gerner, F. M., and Kazmierczak, M., "Analysis of the Heat Transfer Capacity of a Micromachined Loop Heat Pipe," *Proceedings of the ASME*, edited by L. C. Witte, HTD-Vol. 364-3, 1999, pp. 53–60.

[11]Khrustalev, D., "Loop Heat Pipe Technology for Electronics Cooling," *International Conference on High-Density Interconnect and Systems Packaging*, Vol. 4428, Society of Photo-Optical Instrumentation Engineers, Bellingham, WA, 2001, pp. 375–380.

[12]Ku, J., Ottenstein, L., Kaya, T., Rogers, P., and Hoff, C., "Testing of a Loop Heat Pipe Subjected to Variable Accelerations Part 1: Start-Up," Society of Automotive Engineers, Paper 2000-01-2488, July 2000.

[13]Ku, J., Ottenstein, L., Kaya, T., Rogers, P., and Hoff, C., "Testing of a Loop Heat Pipe Subjected to Variable Accelerations Part 2: Temperature Stability," Society of Automotive Engineers, Paper 2000-01-2489, July 2000.

[14]Baker, C., "Geosicence Laser Altimeter System (GLAS) Final Test Report of DM LHP TV Testing," NASA/TP-2000-209898, Dec. 2000.

[15]Wolf, D. A., and Bienert, W. B., "Investigation of Temperature Control Characteristics of Loop Heat Pipes," Society of Automotive Engineers, Paper 941576, June 1994.

[16]Kaya, T., and Ku, J., "Ground Testing of Loop Heat Pipes for Spacecraft Thermal Control," AIAA Paper 99-3447, July 1999.

[17]Kaya, T., and Ku, J., "Investigation of the Temperature Hysteresis Phenomenon of a Loop Heat Pipe," 33rd National Heat Transfer Conf., Paper 108, American Society of Mechanical Engineers, Fairfield, NJ, Aug. 1999.

[18]Ku, J., Ottenstein, L., Rogers, P., and Cheung, K., "Effect of Pressure Drop on Loop Heat Pipe Operating Temperature," 12th International Heat Pipe Conf., Inst. of Thermal Physics of the Russian Academy of Sciences, Ekaterinburg, Russia, May 2002.

[19]Kaya, T., and Hoang, T. T., "Mathematical Modeling of Loop Heat Pipes and Experimental Validation," *Journal of Thermophysics and Heat Transfer*, Vol. 13, No. 3, 1999, pp. 314–320.

[20]Hoang, T. T., and Kaya, T., "Modeling of Loop Heat Pipes with Two-Phase Pressure Drop," AIAA Paper 99-3448, July 1999.

[21]Bienert, W. B., and Wolf, D. A., "Temperature Control with Loop Heat Pipes: Analytical Model and Test Results," *Proceedings of the 9th International Heat Pipe Conference*, Los Alamos National Lab., Albuquerque, NM, 1995.

[22]Cullimore, B., and Baumann, J., "Steady-State and Transient Loop Heat Pipe Modeling," Society of Automotive Engineers, Paper 2000-01-2316, July 2000.

[23]Churchill, S. W., and Chu, H. H. S., "Correlating Equations for Laminar and Turbulent Free Convection from a Vertical Plate," *International Journal of Heat and Mass Transfer*, Vol. 18, No. 11, 1975, pp. 1323–1329.

[24]Morgan, V. T., "The Overall Convective Heat Transfer from Smooth Circular Cylinders," *Advances in Heat Transfer*, edited by T. F. Irvine and J. P. Hartnett, Vol. 11, Academic Press, New York, 1975, pp. 199–264.

[25]Ku, J., Ottenstein, L., Kobel, M., Rogers, P., and Kaya, T., "Temperature Oscillations in Loop Heat Pipe Operation," *American Institute of Physics Conference Proceedings*, No. 552, American Inst. of Physics, New York, Feb. 2001.

[26]Ponnappan, R., Yerkes, K. L., Chang, W. S., and Beam, J. E., "Analysis and Testing of Heat Pipe in Accelerating Environment," *8th International Heat Pipe Conference*, Beijing, 1992, pp. B-19-1–B-19-6.

[27]Kiseev, V. M., Belonogov, A. G., and Belyaev, A. A., "Influence of Adverse Accelerations on the Operation of an Anti-Gravity Heat Pipe," *Journal of Engineering Physics*, Vol. 50, 1986, pp. 394–398.

[28]Nakai, S., and Okazaki, T., "Heat Transfer from Horizontal Circular Wire at Small Reynolds and Grashof Numbers-I, Pure Convection," *International Journal of Heat and Mass Transfer*, Vol. 18, No. 3, 1975, pp. 387–396.